Journal of Controlled Release 282 (2018) 101–109

Contents lists available at ScienceDirect

Journal of Controlled Release

journal homepage: www.elsevier.com/locate/jconrel

Insights into maleimide-thiol conjugation chemistry: Conditions for efficient surface functionalization of nanoparticles for receptor targeting

Lucía Martínez-Jothar[a], Sofia Doulkeridou[b], Raymond M. Schiffelers[c], Javier Sastre Torano[d], Sabrina Oliveira[a,b], Cornelus F. van Nostrum[a], Wim E. Hennink[a,*]

[a] Department of Pharmaceutics, Utrecht Institute for Pharmaceutical Sciences, Utrecht University, Universiteitsweg 99, Utrecht 3584, CG, The Netherlands
[b] Division of Cell Biology, Department of Biology, Utrecht University, Padualaan 8, Utrecht 3584, CH, The Netherlands
[c] Clinical Chemistry and Haematology, University Medical Center Utrecht, Heidelberglaan 100, Utrecht 3584, CX, The Netherlands
[d] Department of Chemical Biology & Drug Discovery, Utrecht Institute for Pharmaceutical Sciences, Utrecht University, Universiteitsweg 99, Utrecht 3584, CG, The Netherlands

ARTICLE INFO

Keywords:
Nanoparticles
PLGA
Maleimide
Targeting
RGD
Nanobody

ABSTRACT

Maleimide-thiol chemistry is widely used for the design and preparation of ligand-decorated drug delivery systems such as poly(lactide-*co*-glycolide) (PLGA) based nanoparticles (NPs). While many publications on nanocarriers functionalized exploiting this strategy are available in the literature, the conditions at which this reaction takes place vary among publications. This paper presents a comprehensive study on the conjugation of the peptide cRGDfK and the nanobody 11A4 (both containing a free thiol group) to maleimide functionalized PLGA NPs by means of the maleimide-thiol click reaction. The influence of different parameters, such as the nanoparticles preparation method and storage conditions as well as the molar ratio of maleimide to ligand used for conjugation, on the reaction efficiency has been evaluated. The NPs were prepared by a single or double emulsion method using different types and concentrations of surfactants and stored at 4 or 20 °C before reaction with the targeting moieties. Several maleimide to ligand molar ratios and different reaction times were studied and the conjugation efficiency was determined by quantification of the not-bound ligand by liquid chromatography. The kind of emulsion used to prepare the NPs as well as the type and concentration of surfactant used had no effect on the conjugation efficiency. Reaction between the maleimide groups present in the NPs and cRGDfK was optimal at a maleimide to thiol molar ratio of 2:1, reaching a conjugation efficiency of 84 ± 4% after 30 min at room temperature in 10 mM HEPES pH 7.0. For 11A4 nanobody the optimal reaction efficiency, 58 ± 12%, was achieved after 2 h of incubation at room temperature in PBS pH 7.4 using a 5:1 maleimide to protein molar ratio. Storage of the NPs at 4 °C for 7 days prior to their exposure to the ligands resulted in approximately 10% decrease in the reactivity of maleimide in contrast to storage at 20 °C which led to almost 40% of the maleimide being unreactive after the same storage time. Our findings demonstrate that optimization of this reaction, particularly in terms of reactant ratios, can represent a significant increase in the conjugation efficiency and prevent considerable waste of resources.

1. Introduction

The capacity of nanoparticulate drug delivery systems to improve the therapeutic index (ratio of efficacy/toxicity) of pharmacologically active compounds, such as drugs and drug candidates as well as protein and nucleic acid based drugs, makes these particles promising systems for the treatment of different diseases. Targeting can be achieved by relying on the physicochemical properties of the drug-loaded nanoparticle and on the anatomy and physiology of the target, leading to accumulation of the drug delivery system mostly on sites with increased permeability of the vascular endothelium, for instance tumors and inflamed tissues [1–4]. Cells of the reticuloendothelial system (e.g. macrophages present in liver and spleen) can also be targeted since they are in charge of the clearance of foreign bodies from the circulation and can easily take up nanocarriers [5–7]. Ligand decorated systems are more suitable for the treatment of pathologies unrelated to the reticuloendothelial system or in which the structure of the endothelium is not compromised. To achieve this, the nanocarrier is functionalized with a ligand that specifically recognizes and interacts with receptors preferably overexpressed on the pathological cells. This in turn can

* Corresponding author.
E-mail address: W.E.Hennink@uu.nl (W.E. Hennink).

https://doi.org/10.1016/j.jconrel.2018.03.002
Received 8 January 2018; Received in revised form 15 February 2018; Accepted 1 March 2018
Available online 09 March 2018

result in an increase in the accumulation and retention of the active principle in the diseased tissue/organ. Since ligand decorated systems are normally internalized by the target cells, they can also be used for the delivery of drugs that do not have the ability to penetrate the cellular membrane by Fickian diffusion, for instance pDNA, siRNA or mRNA [8] as well as therapeutic proteins that have their target intracellularly [9,10]. Although most of the ligand targeted systems currently under clinical evaluation are developed for cancer treatment [11], other applications such as vaccination [12,13] and drug delivery through the blood brain barrier [14,15] are also possible.

As mentioned, receptor-mediated targeting requires the covalent attachment of targeting ligands at the surface of nano-sized delivery vehicles that can be performed by several methods including carbodiimide chemistry [16], reactions with *N*-hydrosuccinimide (NHS) active esters, click chemistry reactions such as azide-alkyne cycloaddition and thiol-ene reaction [17,18], and the use of thiol reactive maleimide groups. The reaction of maleimide derivatives and thiol containing biological molecules was reported > 55 years ago [19,20], but it was not until the early 1980's that its potential as a tool for the functionalization of nanocarriers was shown and exploited [21]. Importantly, the commercial availability of lipids and polymers that contain maleimide groups has enabled the fabrication of liposomes, polymeric nanoparticles, polymeric micelles, polymeric nanogels and polymersomes that can be conjugated to thiol containing ligands to target specific cells or tissues [22–24]. In comparison to more recently developed functionalization strategies, the maleimide-thiol reaction is still frequently applied in functionalization protocols because of the high reactivity of maleimide under mild conditions (i.e. room temperature and aqueous buffers), its selectivity towards thiol groups at physiological pH and the formation of a thioether bond that is relatively stable under most conditions [25]. Additionally, this reaction makes use of the thiol group of cysteine residues naturally present in peptides and proteins or that can be easily introduced in these molecules. However, under certain conditions such as alkaline pH values (pH ≥ 8) [26,27] maleimide is susceptible to hydrolysis resulting in ring opening and formation of a maleic acid amide derivative that is not reactive towards thiol groups [28–30]. Additionally, when maleimide-functionalized building blocks are used in the fabrication of nanocarriers, the preparation method can also have a detrimental effect on the stability of the maleimide groups. For instance, liposome purification by dialysis in PBS (pH 7.0–7.5) for 5 h, resulted in a 50% decrease in maleimide reactivity [31], which highlights the importance of assessing the compatibility of the preparation procedure with the preservation of the structure of maleimide.

Even though maleimide-thiol chemistry has been widely used, the conditions for preparation and functionalization of maleimide containing liposomes and polymer-based drug delivery vehicles, such as poly(lactic acid), poly(ε-caprolactone), or poly(lactic-*co*-glycolic acid) (PLGA) nanoparticles (NPs), often differ widely between publications (Table S1). While this speaks to the robustness of the aforementioned conjugation reaction, it also brings into question the efforts being done to evaluate and optimize the reaction conditions. In this regard, the current work provides an in-depth study of the influence of preparation, handling and functionalization conditions on the reactivity of maleimide groups incorporated in PLGA based nanocarriers. NPs based on blends of PLGA and maleimide- poly(ethylene glycol) $(PEG)_{5000}$-PLGA were chosen as a model formulation due to the well documented and appealing properties of PLGA systems for targeted drug delivery including their biocompatibility, biodegradability, relatively easy production and overall tailorability [32–36]. The last point allows for control of properties such as degradation/release profile, stealth behavior (through the incorporation of PEG chains in the formulation) and, as previously mentioned, decoration of the surface of the particles with targeting moieties. In the present study, two ligands of different molecular weight were chosen, both with potential applications in cancer treatment: cRGDfK and 11A4. cRGDfK is a cyclic peptide (approx. 700 Da) able to target the integrin $\alpha_v\beta_3$ which is overexpressed in some types of tumors including breast cancer and has been correlated with metastasis [37]. The ability of the RGD motif to bind to the aforementioned integrin has been explored as a tool for drug targeting to tumors by preparing drug-RGD conjugates or RGD-targeted carriers [38–41]. Additionally, several radiolabeled RGD peptides for imaging of tumor angiogenesis are currently undergoing clinical trials [42]. The nanobody 11A4 is a C-terminal cysteine modified molecule capable of selectively binding to the HER-2 receptor [43] overexpressed in 15–20% breast cancers [44]. Nanobodies (approx. 15 kDa) are the variable fragments of heavy chain antibodies from camelids [45]. Nanobodies can be easily produced by recombinant technologies and have favorable physicochemical properties, such as high solubility and stability, as well as a relatively small size as compared to full sized antibodies which allows them to efficiently bind to epitopes that are inaccessible to antibodies [46–48].

This paper presents an in-depth study on the functionalization of maleimide-PEG-PLGA NPs with cRGDfK and 11A4 by means of maleimide-thiol conjugation chemistry and explores the influence of the NPs preparation and storage conditions on the efficiency of conjugation. Additionally, reactant ratios and reaction kinetics are studied for both ligands with the objective of identifying the critical parameters and finding the optimal conditions for the maleimide-thiol conjugation reaction.

2. Materials and methods

2.1. Chemicals

PLGA (50:50 ratio DL-lactide/glycolide, IV 0.39 dL/g, Mw ~44,000 Da) was obtained from Purac (Gorinchem, The Netherlands). Methoxy poly(ethylene glycol)-*b*-poly(lactide-*co*-glycolide) (mPEG-PLGA, Mw 5000:20,000 Da) and poly(lactide-*co*-glycolide)-*b*-poly (ethylene glycol)-maleimide (maleimide-PEG-PLGA, Mw 5000:20,000 Da) were purchased from Polyscitech, Akina Inc. (West Lafayette, IN, USA). Poly(vinyl alcohol) (PVA) of Mw 30,000–70,000 Da, 87–90% hydrolyzed, sodium cholate hydrate, dimethyl sulfone ($DMSO_2$) and methoxy poly(ethylene glycol)-maleimide (M_n 2000 Da) were acquired from Sigma-Aldrich. c[RGDfK(Ac-SCH_2CO)] (Mw: 719.8 g/mol) (Fig. S1) was purchased from Peptides International (Louisville, KY, USA).

2.2. Nanoparticle preparation and characterization

Polymeric NPs were prepared using blends of PLGA and maleimide-PEG-PLGA. For particles prepared using the double emulsion solvent evaporation method [49,50], the polymers were dissolved in dichloromethane at 5% w/v of polymer and 4:1 or 9:1 w/w ratio of PLGA and maleimide-PEG-PLGA, respectively. NPs prepared using a 4:1 w/w ratio were used for conjugation with cRGDfK, while those prepared with a 9:1 w/w ratio were used for conjugation with 11A4.

A W/O emulsion consisting of 100 μL of water and 1 mL of the polymer solution was prepared by probe sonication for 1 min at 10% power (SONOPULS HD 2200 Bandelin, Berlin, Germany). This emulsion (1.1 mL) was subsequently added to 10 mL of an external aqueous phase containing either sodium cholate 1% w/v (pH 7.1) or PVA 1, 2.5 or 5% w/v in water. The samples were then sonicated for 2 min at 10% power to form a W/O/W emulsion. The double emulsion method was used for NPs preparation because they are intended for future application as a carrier of hydrophilic molecules. After evaporation of the organic solvent under stirring at room temperature for 2 h, the NPs were collected by centrifugation for 20 min, 20,000 g at 4 °C, washed 2 times with 10 mM HEPES (pH 7.0) and one time with MilliQ water. The NPs were stored in PBS (8.0 g NaCl, 1.15 g Na_2HPO_4, 0.2 g KCl and 0.2 g KH_2PO_4 in 1 L of water, pH 7.4) or HEPES at 4 °C until further use. Control NPs were prepared similarly from a blend of PLGA and mPEG-PLGA in a 4:1 or 9:1 w/w ratio.

Maleimide-PEG-PLGA NPs were also prepared by single emulsion method following a procedure similar as described for the double emulsion. Briefly, PLGA (40 mg) and maleimide-PEG-PLGA (10 mg) were dissolved in 1 mL of dichloromethane (final concentration of polymer 5% w/v), added to 10 mL of an external aqueous phase containing PVA 5% w/v in water and subject to sonication for 2 min at 10%. After evaporation of the solvent the NPs were collected, washed and stored as described for the double emulsion preparation.

The weight fraction of PEG present in the NPs was determined by ^{1}H NMR. PLGA and maleimide-PEG-PLGA in 4:1 or 9:1 w/w ratio respectively, were dissolved in deuterated chloroform ($CDCl_3$). Maleimide-PEG-PLGA NPs prepared by double emulsion method using the procedure described above were freeze dried and dissolved in $CDCl_3$. The blends of PLGA and maleimide-PEG-PLGA of known composition and the NPs were analyzed by ^{1}H NMR and the PEG weight fraction (%) in the samples was determined based on the integrals of the signals of PEG, lactic acid and glycolic acid, as follows [50]:

lactic acid unit

P

The size of the NPs was determined by Dynamic Light Scattering (ALV CGS-3, Malvern) at 25 °C in deionized water and the zeta potential was measured in HEPES 10 mM pH 7.0 at 25 °C (Zetasizer Nano Z, Malvern). An aliquot of NPs suspended in deionized water was freeze dried at −40 °C, < 1 mbar (Christ Alpha 1–2 freeze dryer, Osterode am Harz, Germany).

2.3. Hydrolytic stability of maleimide under NPs preparation conditions

A solution of 0.5 mg/mL of methoxy poly(ethylene glycol)-maleimide in HEPES 10 mM pH 7.0 was treated similarly to the polymer solutions used for NPs preparation. Briefly, 10 mL of the PEGylated maleimide in HEPES was sonicated for 3 min at 10% power (SONOPULS HD 2200 Bandelin, Berlin, Germany) and stirred for 2 h at room temperature. The NPs washing procedure was mimicked by centrifuging the solution for 20 min at 20,000 g and at 4 °C. Four centrifugation cycles were conducted with a waiting time of 20 min between the cycles, which is the approximate time for washing/resuspension of the actual polymeric NPs. Samples of the PEGylated maleimide solution were taken before treatment, directly after sonication and at the end of the procedure (sonication + washings). The maleimide content in the samples was determined by UV absorbance at 302 nm [30,51,52] (Shimadzu UV–Vis Spectrophotometer UV 2450) using a calibration curve obtained by preparing solutions of methoxy poly(ethylene glycol)-maleimide in PBS (pH 7.4) in a concentration range of 0.1–0.8 mg/mL. After UV analysis, the samples were freeze dried, resuspended in deuterium oxide (D_2O) and their PEG content was determined by ^{1}H NMR analysis using $DMSO_2$ as internal standard.

2.4. Preparation of ligands for conjugation to maleimide-PEG-PLGA NPs

Prior to the conjugation reaction, the peptide c[RGDfK(Ac-SCH$_2$CO)] bearing one protected thiol group on the lysine residue (structure of the peptide is shown in Scheme S1) was dissolved in HEPES 10 mM/ethylenediaminetetraacetic acid (EDTA) 0.4 mM (pH 7.0). Deprotection was conducted by addition of 1:10 v/v of deacetylation buffer (HEPES 10 mM/hydroxylamine 0.5 M/EDTA 0.4 mM pH 5.5) (Scheme S1). followed by incubation for 30 min at room temperature [53] (the molecular weight of the deprotected peptide, as determined by LC-MS analysis was 678.5 Da) (Fig. S2).

The 11A4 nanobody bearing a C-terminal cysteine followed by a FLAG tag (theoretical molecular weight 14,813 Da) was produced in BL21 bacteria and purified by protein A affinity chromatography, as described elsewhere [43]. To guarantee the presence of the free thiol on the nanobody, the protein was exposed to reducing conditions for 15 min at room temperature in PBS (8.0 g NaCl, 1.15 g Na_2HPO_4, 0.2 g KCl and 0.2 g KH_2PO_4 in 1 L of water, pH 7.4)/20 mM Tris(2-carboxyethyl)phosphine hydrochloride/0.4 mM EDTA [54]. The reducing agent was removed using Zeba Spin Desalting columns, with buffer exchange to PBS/EDTA 0.4 mM (pH 7.4), before the nanobody was incubated with the NPs.

2.5. Conjugation of cRGDfK and 11A4 to maleimide-PEG-PLGA NPs

The general procedure for the reaction between maleimide-PEG-PLGA NPs and the targeting ligands was the following: a NPs suspension (prepared by either single emulsion using 5% w/v PVA or by double emulsion using sodium cholate 1% w/v or PVA 1, 2.5 or 5% w/v) was prepared in deionized water and its concentration was determined by taking an aliquot and freeze drying it overnight at −40 °C, < 1 mbar (Christ Alpha 1–2 freeze dryer, Osterode am Harz, Germany). The NPs suspensions of known concentration were used to prepare NPs samples for reaction with the targeting ligands. For example, aliquots containing 1 or 3 mg of NPs were taken from the NPs suspension and their volume was adjusted to 300 μL with PBS (8.0 g NaCl, 1.15 g Na_2HPO_4, 0.2 g KCl and 0.2 g KH_2PO_4 in 1 L of water, pH 7.4)/0.4 mM EDTA, or to 600 μL using HEPES (pH 7.0)/0.4 mM EDTA, respectively. The samples prepared in HEPES were used for reaction with cRGDfK and those prepared with PBS for reaction with 11A4.

The NPs suspensions were incubated with cRGDfK at molar ratios 3:1, 2:1 and 1:1 of maleimide-PEG-PLGA to peptide, or with 11A4 at molar ratios of 20:1, 10:1, 5:1, 2:1 and 1:1 of maleimide-PEG-PLGA to protein. As an example, for the 1:1 ratio maleimide-PEG-PLGA to 11A4, 59 μg of protein was used for conjugation with 1 mg of NPs; while for 1:1 ratio maleimide-PEG-PLGA to cRGDfK, 5 μg of peptide was used for conjugation with 1 mg of NPs. The samples were placed on a nutating mixer and after incubation at room temperature, pH 7.0–7.4 (for cRGDfK and 11A4 respectively), for 2 h (unless stated otherwise), the NPs were recovered by centrifugation for 10 min, 3000 g, 4 °C, and washed once with PBS. The unbound ligands present in the supernatants were quantified by HPLC (for cRGDfK) or UPLC (for 11A4) as described in the section Quantification of cRGDfK and 11A4 by HPLC or UPLC to determine the conjugation efficiencies. Based on the obtained results, the maleimide-PEG-PLGA to ligand molar ratios resulting in highest conjugation efficiencies, namely 2:1 for cRGDfK and 5:1 for 11A4, were chosen for other tests.

The influence of the NPs preparation conditions on the efficiency of the maleimide – thiol reaction was evaluated by conjugating cRGDfK to NPs prepared by a single or double emulsion method. The influence of the surfactant used for NPs preparation on the conjugation efficiency was also studied by conjugating cRGDfK and 11A4 to NPs prepared by a double emulsion method using either sodium cholate 1% w/v or PVA 1, 2.5 or 5% w/v. Conjugation was done at maleimide to ligand molar ratios of 2:1 for cRGDfK and 5:1 for 11A4.

To obtain insight into the reaction kinetics, the targeting ligands cRGDfK and 11A4 were incubated with maleimide-PEG-PLGA NPs at 2:1 and 5:1 maleimide to ligand molar ratios respectively, for different times (5 min to 16 h), after which the samples were placed in an ice bath and subsequently centrifuged (3000 g, 10 min, 4 °C) in order to recover and quantify the unbound ligand by HPLC as detailed in the section Quantification of cRGDfK and 11A4 by HPLC or UPLC to determine the conjugation efficiencies.

For determining the stability of the maleimide groups, PLGA NPs containing 20% maleimide-PEG-PLGA were stored either at 4 °C or room temperature (~20 °C) in buffer HEPES 10 mM/EDTA 0.4 mM (pH 7.0) for 1 to 7 days, after which they were subjected to conjugation with cRGDfK at a 2:1 maleimide to ligand molar ratio as described above. The stability of maleimide was calculated by comparing the

conjugation efficiency obtained immediately after NPs preparation (T_0) to the ones found at the subsequent incubation times.

2.6. Quanti cation of cRGDfK and 11A4 by HPLC or UPLC to determine the conjugation e ciencies

Deprotected cRGDfK was quantified by HPLC (Waters Alliance System) using a XBridge BEH C18 column (3.5 µm, 100 mm × 2.1 mm, Waters) and a gradient from 100% eluent A (5.0% ACN, 94.9% water, 0.1% acetic acid) to 75% eluent B (94.5% ACN, 5.0% water, 0.1% acetic acid) over 12 min, and subsequently 100% eluent B for 1 min. The injection volume was 50 µL and the peptide was detected by absorbance at 214 nm (detection limit was 2 µg/mL). Standard solutions of deprotected cRGDfK (2–30 µg/mL in HEPES 10 mM/EDTA 0.4 mM) were used for calibration (Fig. S3).

Quantification of 11A4 was performed by UPLC (Acquity UPLC) using a BEH C4 300 Å column (1.7 µm, 50 mm × 2.1 mm, Waters) using a gradient from 100% eluent A (5.0% ACN, 94.9% water, 0.1% trifluoroacetic acid) to 100% eluent B (99.9% ACN, 0.1% trifluoroacetic acid) over 5 min (Fig. S4). The injection volume was 7.5 µL, the protein was detected by fluorescence (excitation at 280 nm, emission at 340 nm) and the detection limit was 5 µg/mL. Standard solutions of 11A4 (5–100 µg/mL in PBS/EDTA 0.4 mM) were used for calibration (Fig. S5).

The conjugation efficiency was calculated as follows:

$$\frac{-}{-} \quad 100\%$$

Ligand in the supernatant is the sum of the amount of cRGDfK or 11A4 found in the supernatant after recovery of the NPs at the end of the conjugation reaction and the amount of ligand found in the solution used to wash the NPs pellet. As controls, NPs prepared from a blend of PEG-PLGA and PLGA (thus lacking maleimide groups) were exposed to cRGDfK or 11A4 under the same conditions as NPs containing maleimide groups.

3. Results and discussion

3.1. Nanoparticle preparation

Maleimide functionalized PEG-PLGA NPs were prepared by emulsification of dichloromethane solutions of PLGA and maleimide-PEG-PLGA in an aqueous phase containing PVA or sodium cholate as surfactant and subsequent evaporation of the solvent. The NPs were washed and collected by centrifugation, and the chemical composition of the isolated nanoparticles was analyzed by ^{1}H NMR (Fig. S6A). Additionally, the PEG signal can be detected by ^{1}H NMR after NPs suspension in D_2O (Fig. S6B). The PEG peak for NPs suspended in D_2O is broader as compared to those dissolved in $CDCl_3$, which can be explained by a reduced mobility of the PEG chains anchored to the surface of the NPs [55–57]. The weight fraction of PEG in the NPs was determined by ^{1}H NMR analysis of blends of PLGA and maleimide-PEG-PLGA (4:1 or 9:1 w/w ratio, respectively) and of NPs dissolved in $CDCl_3$ (Fig. S7). This analysis confirmed the quantitative incorporation of maleimide-PEG-PLGA in the NPs (Table S2).

The NPs prepared had diameters in the range of 300–360 nm, with larger sizes being observed for NPs with higher maleimide-PEG-PLGA content. The size distributions were narrow as reflected by the low PDI values (~0.1). Slightly negative zeta potentials (~ − 7.0 mV) were obtained for both types of NPs (Table S3), which can be explained by the shielding of the negatively charged carboxyl end groups of PLGA (uncapped polymer).

3.2. Hydrolytic stability of maleimide under NPs preparation conditions

Possible hydrolysis of maleimide (Fig. S8) can be followed by UV–Vis spectroscopy [30,52] since as a cyclic imide it absorbs at ~300 nm while its hydrolysis product, maleamic acid, lacks absorbance at this wavelength [51]. To investigate whether the NPs preparation method results in the hydrolysis of maleimide groups, PEG-maleimide in an aqueous buffer was subjected to similar conditions as those used for NPs preparation (i.e. sonication and incubation at pH 7.0 and 20 °C for 2–5 h) and the maleimide content was monitored at 302 nm. Compared to the PEGylated maleimide control (sample not subjected to sonication or mimicking of the washings), the concentration of maleimide in the treated samples decreased only by 15 ± 1% (n = 2) under the experimental conditions. ^{1}H NMR analysis of the samples in D_2O, using $DMSO_2$ as internal standard, confirmed that the PEG content remained constant in the samples during the procedure, which indicates that the decrease in the UV signal of maleimide can be attributed to its hydrolysis and not to a decrease in the concentration of PEG-maleimide e.g. precipitation of the product. Since the decrease in the signal of maleimide became apparent after sonication, and because the rate of hydrolysis is known to increase at higher temperatures [52], the hydrolysis of maleimide is likely caused by an increase in temperature during sonication of the sample.

3.3. Characterization of maleimide-PEG-PLGA NPs functionalized with cRGDfK or 11A4

The size and charge of PEG-PLGA NPs and maleimide-PEG-PLGA NPs was monitored before and after incubation with cRGDfK and 11A4 (Table 1). The negative control consisting of NPs containing mPEG-PLGA without maleimide functionalities did not show conjugation nor binding of either cRGDfK or 11A4, while both ligands could effectively be coupled to the NPs containing maleimide-PEG-PLGA. This finding shows that the functionalization of NPs is indeed established via the chemical conjugation reaction between maleimide and the thiol group

Table 1
Size, zeta potential and conjugation efficiency of polymeric NPs of different compositions[a] incubated with cRGDfK and 11A4[b].

PEGylated polymer content (%w/w)	Ligand used for conjugation	Diameter (nm)	PDI	Zeta potential (mV)	Conjugation efficiency (%)
10% PEG-PLGA	None	296 ± 9	0.09 ± 0.02	−7.0 ± 0.3	NA
10% PEG-PLGA	11A4	309 ± 5	0.09 ± 0.07	−6.7 ± 0.4	0
10% maleimide-PEG-PLGA	None	294 ± 5	0.10 ± 0.01	−7.5 ± 0.3	NA
10% maleimide-PEG-PLGA	11A4	311 ± 1	0.08 ± 0.01	−13.6 ± 0.8	45
20% PEG-PLGA	None	322 ± 4	0.03 ± 0.00	−5.7 ± 0.2	NA
20% PEG-PLGA	cRGDfK	329 ± 5	0.03 ± 0.01	−5.8 ± 0.3	0
20% maleimide-PEG-PLGA	None	356 ± 4	0.15 ± 0.02	−8.4 ± 0.3	NA
20% maleimide-PEG-PLGA	cRGDfK	353 ± 6	0.10 ± 0.01	−9.1 ± 0.0	86

[a] NPs prepared by double emulsion method, n = 1.
[b] Conjugation reaction performed in molar ratios of 2:1 maleimide-polymer to cRGDfK and 5:1 maleimide-polymer to 11A4.

present in the ligands and not by physical interactions.

Conjugation of the cyclic peptide cRGDfK to the maleimide-PEG-PLGA NPs did not significantly alter their size and zeta potential. Similar zeta potentials for nanoparticles before and after conjugation to RGD derivatives have also been reported by other authors [58,59].

The diameter of NPs decorated with 11A4 was almost 20 nm larger than the particles before conjugation and a slight increase in PDI for the former was also observed. The dimensions of the nanobody are 3 × 3 × 4 nm [60] and therefore its attachment to the surface of the NPs can be expected to result in an increase in their hydrodynamic diameter of up to 10 nm, which is close to the increase observed for the NPs. Most notably, the zeta potential of the NPs became more negative after conjugation to 11A4. The pI of 11A4 (determined by the ExPASy ProtParam Tool) is 7.94, which would confer a slightly positive charge under the conditions tested (pH 7.4). Nonetheless, this value refers to the charge of the nanobody based on its amino acid sequence, while in reality the folded form of the protein is present on the NPs surface, meaning that the amino acid residues exposed to the medium may actually result in an overall negative charge.

3.4. Conjugation of cRGDfK and 11A4 to maleimide-PEG-PLGA NPs: e ect of maleimide-PEG-PLGA to ligand molar ratio

One of the main parameters to consider for functionalization of maleimide-PEG-PLGA NPs is the molar ratio between the ligand and the reactive surface group. However, authors seldom report optimization studies for their formulation and, in some cases, the molar ratios of maleimide to ligand used for the reaction are not even reported (see Table S1). In this work, the relationship between the ratios of reactants and the coupling efficiency was evaluated by conjugating cRGDfK and 11A4 to maleimide-PEG-PLGA NPs at different maleimide polymer to ligand molar ratios. For this set of experiments, as well as all others described from here on, NPs with 10 and 20% w/w maleimide-PEG-PLGA were prepared which were subsequently incubated with 11A4 and cRGDfK, respectively. For conjugation of cRGDfK we chose a higher maleimide content since this peptide is much smaller than the nanobody and occupies less space on the surface of the NPs. The efficiencies of the conjugation reaction are shown in Fig. 1.

At a molar excess of maleimide units, and equal reaction time (2 h), higher maximum conjugation efficiencies were observed for cRGDfK (almost 100% at a molar ratio of 3 maleimide-PEG-PLGA to 1 cRGDfK as compared to 11A4 (around 70% at a 20:1 ratio), which can be explained by the larger size of the protein compared to that of the peptide. The thiol group of cRGDfK is present on the lateral chain of a lysine residue (Scheme S1) and is therefore present on the outside of the cyclic structure, which makes it excellently accessible for reaction with the

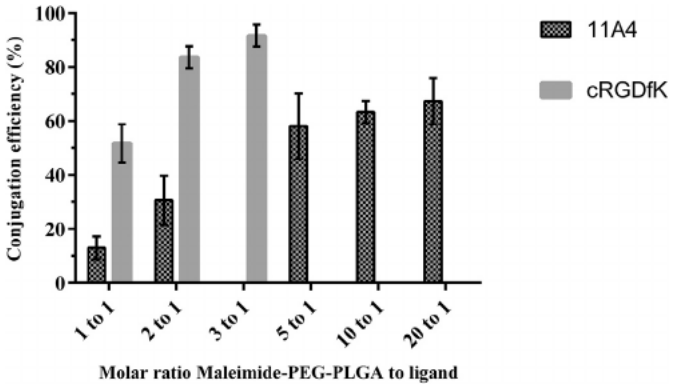

Fig. 1. Conjugation efficiencies (%) at different maleimide-PEG-PLGA to ligand molar ratios. Conjugation efficiency to cRGDfK and 11A4 (n = 3, except for 11A4 1:1 ratio). NPs containing 10% maleimide-PEG-PLGA were used for conjugation to 11A4 and NPs with 20% maleimide-PEG-PLGA were used for reaction with cRGDfK. NPs were prepared using the double emulsion solvent evaporation method.

maleimide groups present on the surface of the NPs. In line with our observations, high conjugation efficiencies (> 95%) have been previously reported for cRGDfK to liposomes and to maleimide-PEG-poly (lactic acid) NPs when using an excess of maleimide [53,61].

Fig. 1 also shows that with an increasing amount of peptide or protein with respect to maleimide units, a decrease in conjugation efficiency was observed. For the nanobody, the use of a 5:1 maleimide to protein molar ratio during the reaction resulted in a conjugation efficiency of 58 ± 12%. In contrast, at equimolar or even a two-fold excess of maleimide the coupling efficiency was 13 ± 4% and 31 ± 9% respectively. The bulkier nature of the 11A4 molecules already bound to the NPs surface very likely hinder accessibility of unbound protein present in the bulk to neighboring coupling sites. In other words, a more cost-effective preparation of protein-targeted drug delivery systems can be achieved when the stoichiometry is optimized and in this case a larger excess (5:1) of maleimide in respect to 11A4 is used. For a smaller ligand like cRGDfK steric hindrance is less likely to have a large impact on the efficiency of the reaction and at a 1:1 ratio of cRGDfK peptide to maleimide, 52 ± 7% of the peptide was conjugated. Taking into account that ~90% of the PEG-maleimide used for NPs preparation was incorporated (Table S2) and that the NPs preparation method does not result in significant hydrolysis of maleimide groups (see section Hydrolytic stability of maleimide under NPs preparation conditions), it can be concluded that either not all maleimide groups were available for conjugation or that the surface of the NPs is fully covered with peptides at a conjugation ratio 2:1. The preparation of (nano)particles by adding amphiphilic PEGylated block copolymers to the feed relies on the principle that PEG migrates to the particle/water interface and will form a structure consisting of a hydrophobic PLGA core and a shell of PEG chains. However, due to the miscibility of PEG and PLGA [62–64], the core likely also contains PEG. Additionally, the presence of aqueous domains inside the particles resulting from the W/O/W emulsion method could also lead to solubilization of PEG chains in their core [65], which means that not all PEG chains present in the NPs are exposed on the surface. Indeed, considering that almost full conjugation is achieved at a 2:1 molar ratio (84 ± 4%) while lower efficiencies are observed at a 1:1 molar ratio (52 ± 7%), we can speculate that about 50–60% of the maleimide-PEG-PLGA used for NPs preparation is actually available for conjugation on the NPs surface.

An estimation of the number of ligands on the surface of a NP can be obtained by calculating the surface area of a NP, the number of NPs and the surface concentration of ligand (based on the conjugation efficiency) (Calculations S1 and Calculations S2).

It is calculated that for a conjugation reaction between NPs and cRGDfK at a maleimide to peptide molar ratio of 3:1 almost 40,000 ± 5100 peptides were present per NP. The number of cRGDfK molecules per NP further increased to ~50,600 ± 2600 and ~62,500 ± 8600 for the 2:1 and 1:1 ratios respectively (Fig. 2A). Despite the presence of two times more peptide in the reaction at a 1:1 ratio compared to that at 2:1, the number of cRGDfK molecules per NP increased only by a factor ~1.2, which could be an indication of either the saturation of binding sites (maleimide) present per NP or a complete coverage of the NP surface.

For NPs conjugated with 11A4 at a molar ratio of 20:1 an average of ~1600 ± 200 molecules of 11A4 per NP was calculated (Fig. 2B). This amount nearly doubled at the ratio 10:1 (~3000 ± 200) and was almost 3.5 fold higher at the ratio 5:1 (~5500 ± 1200). At ratios of 2:1 and 1:1 no further increase in number of 11A4 molecules was observed, indicating that the at a ratio of 5:1 the surface of the NPs is fully covered with nanobody molecules.

Based on the information from Fig. 2, it is possible to estimate the surface area occupied by one molecule of ligand (Calculations S1 and Calculations S2). For cRGDfK, after reaction at a molar ratio of 3:1 one molecule occupies 10 nm^2 and 6 nm^2 when the ratio is increased to 1:1. In the case of 11A4, a molecule of nanobody is calculated to be present per 197 nm^2 at a reaction ratio of 20:1 and 49 nm^2 at 1:1, which is quite

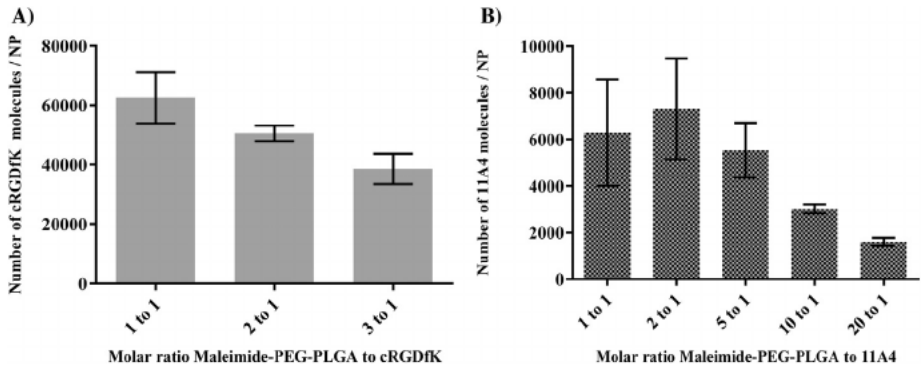

Fig. 2. Number of A) cRGDfK or B) 11A4 molecules conjugated to the surface of one NP at different conjugation ratios.

similar to the data obtained for the ratios 2:1 and 5:1 (46 and 59 nm^2, respectively). Based on the dimensions of the nanobody (3 × 3 × 4 nm) [60], the surface area that one nanobody in an adsorbed monolayer would occupy on the surface of a NP can be calculated as ~12 nm^2. The area occupied by the nanobody according to the calculations is 4–5 fold larger, which can be explained by the fact the protein is coupled to a very flexible PEG_{5000} chain. Therefore, for entropic reasons full surface coverage will not be obtained. Furthermore, depending on the PEG density on the NPs surface, PEG chains can adopt different configurations (i.e. brush or mushroom) which will occupy different surface areas on the NPs [65–67].

The optimal maleimide to ligand molar ratios for reaction, 2 to 1 for cRGDfK and 5 to 1 for 11A4, were used in the experiments described in the following sections of this manuscript. The experiments in which the parameters tested are not expected to be influenced by the size of the ligand were conducted only with cRGDfK because of the higher conjugation efficiencies obtained for this peptide (84 ± 4%) as compared to the nanobody (58 ± 12%) at the optimal ratios for reaction.

3.5. Kinetics of the conjugation reaction between maleimide-PEG-PLGA NPs and cRGDfK or 11A4

The kinetics of the conjugation reaction of the targeting ligands and the polymeric NPs was determined with particular interest in finding the point at which the reaction is complete. Fig. 3A shows that reaction kinetics were particularly fast for cRGDfK, i.e. > 65% of the ligand had already reacted with the maleimide groups on the NPs within the first 5 min of incubation and conjugation reached a plateau value upon 30 min of incubation (around 80% conjugation efficiency for 2:1 maleimide to cRGDfK molar ratio). A longer incubation time of ~16 h did not result in a further increase in conjugation efficiency. Similar fast reaction kinetics, consistent with those found for cRGDfK, have been previously reported between maleimide derivatives and other small thiol containing molecules. For instance, completion of the reaction between maleimide or *N*-ethylmaleimide and L-cysteine in solution is reached in < 2 min [68], with similar results being obtained for the reaction between a carboxy-PEG maleimide derivative and 2-mercaptoethanol, L-cysteine and the peptide CGIRGERA [69]. In the aforementioned cases the reaction reaches completion at faster rates than those observed in the present study, which is expected since faster reaction rates, attributable to diffusional effects, have been observed for systems in which the reactants are soluble in the reaction media as opposed to at least one of them being anchored to a solid particle, for instance liposomes [69] and resin beads [70,71].

The kinetics of the reaction between 11A4 and maleimide-PEG-PLGA NPs are presented in Fig. 3B. A relatively slow and steady increase in the amount of protein conjugated to the NPs was observed during the first 2 h of incubation, after which the maximum coupling efficiency was reached (55% at a 5:1 maleimide to 11A4 molar ratio). Similar to cRGDfK, incubation times longer than 2 h did not result in increased conjugation efficiency of the protein. In comparison to cRGDfK, 11A4 exhibited slower reaction kinetics, which is not surprising since the reaction rate is dependent on the diffusion coefficient of the reactants in the medium which, in its turn, is dependent on their size and shape. cRGDfK, being a cyclic structure that is > 20 times smaller than 11A4, consequently has a larger diffusion coefficient than the latter. When using maleimide-thiol chemistry for functionalization of drug delivery systems authors often favor long reaction times, for instance ≥ 9 h (Table S1). Such long incubations may not be necessary since, according to our findings, the kinetics for coupling of a ligand to a polymeric NPs system are relatively fast, with reaction completion in a time frame of 30 min (peptide) to 2 h (nanobody).

3.6. Influence of the NPs preparation method on maleimide accessibility and conjugation efficiency

The efficiency of the functionalization of maleimide-PEG-PLGA NPs with cRGDfK and 11A4 does not only rely on the reactivity of the

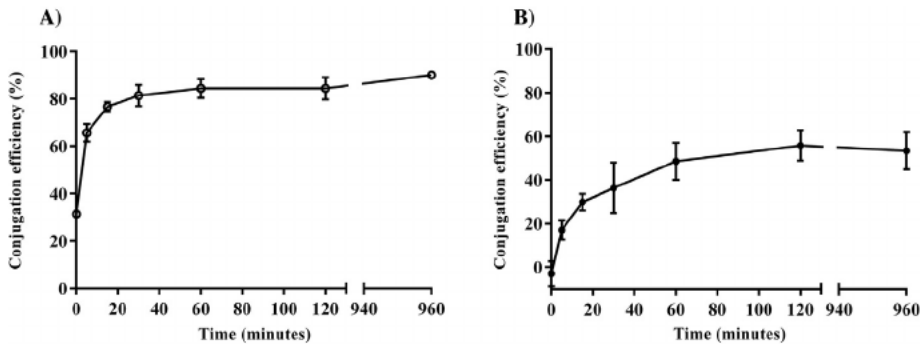

Fig. 3. Kinetics of the conjugation reaction between maleimide-PEG-PLGA NPs and A) cRGDfK (n = 3) or B) 11A4 (n = 2). t = 0 corresponds to the addition of the ligand to the NPs suspension immediately followed by a 10 min centrifugation cycle at 4 °C.

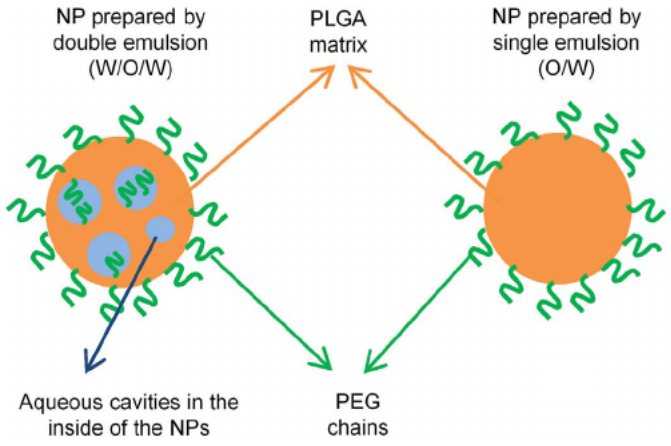

Fig. 4. Schematic illustration of PEG-PLGA NPs prepared by double (W/O/W) and single (O/W) emulsion methods.

maleimide group, but also on its accessibility for reaction with the thiol containing molecule, which in turn is most likely dependent on the NPs preparation procedure. Emulsification methods are commonly used for the preparation of PLGA NPs and the choice of single or double emulsion depends mostly on the nature of the cargo, i.e. whether it is hydrophobic or hydrophilic, respectively, though for amphiphilic drugs both options could be explored [33,72,73]. In an O/W emulsion the drug is dissolved or dispersed in a solution of PLGA in a suitable solvent like dichloromethane or chloroform. This solution is subsequently emulsified in water resulting in the formation of drug-loaded particles upon evaporation of the volatile solvent. In a W/O/W emulsion procedure water droplets containing the drug are emulsified in the organic phase that in turn is dispersed in an external aqueous phase. When PEGylated PLGA is present, one could hypothesize that, due to the presence of aqueous cavities inside the particles prepared by double emulsion, PEG chains could remain entrapped in said cavities due to their hydrophilic nature and thereby not be exposed to the outer surface. This phenomenon is not expected for particles prepared by O/W emulsion since a hydrophobic/hydrophilic interface is only present at the outer surface (Fig. 4).

To investigate the hypothesis that the NPs prepared by the single emulsion method have more maleimide groups exposed at the surface than NPs prepared by the double emulsion method, both procedures were used to prepare NPs which were subsequently reacted with cRGDfK in a 2:1 maleimide-polymer to thiol molar ratio. The results however showed that cRGDfK was conjugated to the NPs to the same extent regardless of the preparation method: 81 ± 4% and 79 ± 4% for the NPs prepared by W/O/W and O/W respectively (n = 2). This suggests that the number of PEG and consequently of maleimide molecules located on the surface of the NPs is not influenced by the type of emulsion used for their preparation. Our data are consistent with a previous report in which analysis of the surface PEG content by ^{1}H NMR in D_2O showed comparable PEG coating efficiencies for NPs prepared by single and double emulsion methods [74]. Since PEG and PLGA are miscible [62–64], it is possible that PEG chains that are not located on the surface of the NPs are dissolved in the polymeric matrix to a similar extent for the NPs prepared by both single (O/W) and double (W/O/W) emulsion methods. Since the NPs preparation method does not influence the conjugation efficiency, and because the nanoparticulate system described in this manuscript is intended for future use as a vehicle for molecules of hydrophilic nature, the double emulsion solvent evaporation method used in previous sections was also chosen for preparation of the NPs used in the experiments described in the next sections.

3.7. Influence of the surfactant used for NPs preparation on conjugation efficiency

A surfactant that adequately stabilizes the emulsion is a key component in the preparation of NPs by emulsification methods. While PVA is one of the preferred surfactants because it allows for the preparation of relatively small NPs with a narrow size distribution, its complete removal from the formulation after preparation is often difficult [75,76]. Residual PVA associated to the surface of polymeric NPs can range from 5 to 20% depending, among others, on the concentration of the surfactant used [49,77]. PVA can modify the properties of the NPs by altering their charge, their degradation profile and even their interaction with and uptake by living cells [78]. It is therefore imaginable that PVA associated to the NPs could also affect their functionalization by partly masking the maleimide groups present on their surface, limiting accessibility and hindering its reaction with thiol containing ligands. In order to investigate whether the type and concentration of surfactant used in the formulation have an influence on its functionalization, NPs were prepared using either sodium cholate, an anionic surfactant which can be almost completely washed off from NPs surface [79], or different concentrations of PVA.

The results shown in Table 2 indicate that the conjugation of cRGDfK to maleimide-PEG-PLGA NPs was not affected by either the nature (ionic or nonionic) or the concentration of the surfactants used for NPs preparation. Because cRGDfK is a small molecule, it can be argued that it could find the space to reach and react with maleimide even in the presence of PVA. Therefore, the conjugation reaction was repeated with 11A4, which has a molecular weight ~20 times larger than that of cRGDfK. In line with the findings for cRGDfK, the conjugation efficiency for 11A4 was, albeit lower, also not significantly dependent on the type and concentration of surfactant used to prepare the formulation (Table 2). It can therefore be concluded that in the conditions used for NPs preparation (which include 3 washing steps), the possible residual PVA present on the surface of the NPs did not affect the extent of ligand conjugation when compared to sodium cholate.

3.8. Preservation of the reactivity of maleimide upon NPs storage as aqueous dispersion at different temperatures

Hydrolysis of maleimide (Fig. S8) may not only occur during preparation, but also upon storage of the NPs before the conjugation reaction. A direct, practical approach to study possible hydrolysis of this functional group during storage of the NPs is through its reaction with thiol containing ligands. For this purpose, maleimide-PEG-PLGA NPs were stored in buffer of pH 7.0 at either room temperature (~20 °C) or 4 °C for different periods of time after which they were subject to conjugation with the peptide cRGDfK in a 2:1 maleimide to peptide molar ratio. Conjugation of the peptide to the NPs immediately after their preparation (t_0, no storage) resulted in 85% conjugation efficiency and was used as reference for the other time points. As shown in Fig. 5, NPs stored at room temperature showed a more rapid decrease in conjugation efficiency towards cRGDfK than those stored at 4 °C. Relative to t_0 around 90% of the maleimide groups remained reactive after

Table 2
Conjugation of cRGDfK and 11A4 to maleimide-PEG-PLGA NPs prepared using different types and concentrations of surfactant (n = 1).

Surfactant used for NPs preparation (% w/v in the external phase)	Conjugation efficiency(%)	
	cRGDfK	11A4
Sodium cholate 1.0	87	44
PVA 1.0	86	49
PVA 2.5	83	50
PVA 5.0	86	52

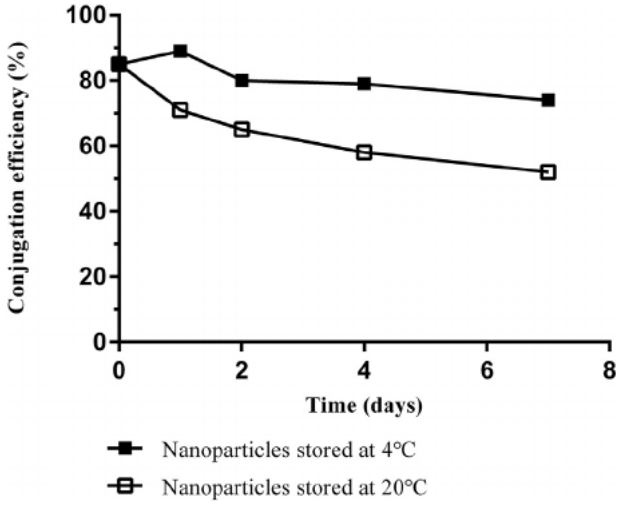

Fig. 5. Reactivity of maleimide groups in NPs upon storage. Maleimide-PEG-PLGA NPs were stored in aqueous medium (HEPES 10 mM pH 7.0) at 4 or 20 °C for different periods of time after which the reactivity of maleimide was assessed by conjugation to cRGDfK.

storage at 4 °C for up to 7 days. In contrast, for the samples kept at room temperature reactivity decreased by 15% already after 1 day of storage and continued to drop over time, with approximately 40% of maleimide being unreactive after 7 days. Based on the information obtained from this study, half-life of maleimide on the NPs is estimated at 32 days when stored at 4 °C and 11 days at 20 °C (Fig. S9 and Table S4) showing that the effect of storage conditions on maleimide hydrolysis cannot be neglected. Likewise, other authors have studied the stability of a maleimide derivative (8armPEG$_{10,000Da}$-maleimide) under different conditions and found that the percentage of hydrolyzed maleimide groups increased with increasing incubation temperatures [52].

4. Conclusions

The findings presented in this work demonstrate the relevance of exploring and optimizing the reaction conditions (i.e. time and stoichiometric ratio) used for functionalization of nanoparticles by maleimide-thiol click reaction, a matter of interest considering that the availability of ligands can often be limited for technical or economic reasons. In this study, the efficiency of the conjugation reaction between maleimide-PEG-PLGA NPs and biomolecules of two different sizes (a 678 Da peptide and a 14.8 kDa protein) was particularly susceptible to the molar ratios used, one of the parameters that was optimized in the present study. As the molar ratio of ligand/maleimide increases, it is likely that saturation of the surface area of the NPs becomes the limiting factor for achieving a high coupling efficiency, which is particularly evident for the larger ligand used in the present study (11A4 nanobody). Identifying the molar ratio at which surface saturation occurs is important in order to avoid the use of excessive amounts of ligand that will not be grafted on the surface of the NPs and will ultimately be discarded in the unbound fraction. In addition to a better use of resources, optimization of the conjugation process results in a better knowledge of the composition of ligand-targeted systems, for instance the surface density of targeting ligand. The structure of the surface of these systems very likely influences their interaction with cells and therefore their performance in vitro and in vivo (i.e. circulation kinetics of NPs and their uptake by cells).

Acknowledgements

Lucía Martínez-Jothar would like to thank the Consejo Nacional de Ciencia y Tecnología (CONACyT), Mexico (grant no. 384743) for the financial support during her PhD.

Appendix A. Supplementary data

Supplementary data to this article can be found online at https://doi.org/10.1016/j.jconrel.2018.03.002.

References

[1] V.P. Torchilin, Drug targeting, Eur. J. Pharm. Sci. 11 (2000) S81–S91.
[2] J. Fang, H. Nakamura, H. Maeda, The EPR effect: unique features of tumor blood vessels for drug delivery, factors involved, and limitations and augmentation of the effect, Adv. Drug Deliv. Rev. 63 (2011) 136–151.
[3] H. Nehoff, N.N. Parayath, L. Domanovitch, S. Taurin, K. Greish, Nanomedicine for drug targeting: strategies beyond the enhanced permeability and retention effect, Int. J. Nanomedicine 9 (2014) 2539–2555.
[4] S. Kunjachan, R. Pola, F. Gremse, B. Theek, J. Ehling, D. Moeckel, B. Hermanns-Sachweh, M. Pechar, K. Ulbrich, W.E. Hennink, G. Storm, W. Lederle, F. Kiessling, T. Lammers, Passive versus active tumor targeting using RGD- and NGR-modified polymeric nanomedicines, Nano Lett. 14 (2014) 972–981.
[5] I. Brigger, C. Dubernet, P. Couvreur, Nanoparticles in cancer therapy and diagnosis, Adv. Drug Deliv. Rev. 54 (2002) 631–651.
[6] D.E. Owens, N.A. Peppas, Opsonization, biodistribution, and pharmacokinetics of polymeric nanoparticles, Int. J. Pharm. 307 (2006) 93–102.
[7] M.J. Ernsting, M. Murakami, A. Roy, S.D. Li, Factors controlling the pharmacokinetics, biodistribution and intratumoral penetration of nanoparticles, J. Control. Release 172 (2013) 782–794.
[8] U. Lachelt, E. Wagner, Nucleic acid therapeutics using polyplexes: a journey of 50 years (and beyond), Chem. Rev. 115 (2015) 11043–11078.
[9] D. Li, C.F. van Nostrum, E. Mastrobattista, T. Vermonden, W.E. Hennink, Nanogels for intracellular delivery of biotherapeutics, J. Control. Release 259 (2017) 16–28.
[10] J. Chen, J. Ouyang, Q. Chen, C. Deng, F. Meng, J. Zhang, R. Cheng, Q. Lan, Z. Zhong, EGFR and CD44 dual-targeted multifunctional hyaluronic acid nanogels boost protein delivery to ovarian and breast cancers in vitro and in vivo, ACS Appl. Mater. Interfaces 9 (2017) 24140–24147.
[11] R. van der Meel, L.J. Vehmeijer, R.J. Kok, G. Storm, E.V. van Gaal, Ligand-targeted particulate nanomedicines undergoing clinical evaluation: current status, Adv. Drug Deliv. Rev. 65 (2013) 1284–1298.
[12] M.D. Joshi, W.J. Unger, G. Storm, Y. van Kooyk, E. Mastrobattista, Targeting tumor antigens to dendritic cells using particulate carriers, J. Control. Release 161 (2012) 25–37.
[13] D.J. Irvine, M.C. Hanson, K. Rakhra, T. Tokatlian, Synthetic nanoparticles for vaccines and immunotherapy, Chem. Rev. 115 (2015) 11109–11146.
[14] M. Pinzon-Daza, I. Campia, J. Kopecka, R. Garzon, D. Ghigo, C. Rigant, Nanoparticle- and liposome-carried drugs: new strategies for active targeting and drug delivery across blood-brain barrier, Curr. Drug Metab. 14 (2013) 625–640.
[15] I. van Rooy, E. Mastrobattista, G. Storm, W.E. Hennink, R.M. Schiffelers, Comparison of five different targeting ligands to enhance accumulation of liposomes into the brain, J. Control. Release 150 (2011) 30–36.
[16] N. Nakajima, Y. Ikada, Mechanism of amide formation by carbodiimide for bioconjugation in aqueous media, Bioconjug. Chem. 6 (1995) 123–130.
[17] M. van Dijk, D.T.S. Rijkers, R.M.J. Liskamp, C.F. van Nostrum, W.E. Hennink, Synthesis and applications of biomedical and pharmaceutical polymers via click chemistry methodologies, Bioconjug. Chem. 20 (2009) 2001–2016.
[18] M. King, A. Wagner, Developments in the field of bioorthogonal bond forming reactions-past and present trends, Bioconjug. Chem. 25 (2014) 825–839.
[19] E. Friedmann, D.H. Marrian, I. Simon-Reuss, Antimitotic action of maleimide and related substances, Br. J. Pharmacol. 4 (1949) 105–108.
[20] C.C. Lee, E.R. Samuels, Adducts from the reaction of N-ethylmaleimide with L-cysteine and with gluthatione, Can. J. Chem. 39 (1961) 1152–1154.
[21] F.J. Martin, D. Papahadjopoulos, Irreversible coupling of immunoglobulin fragments to preformed vesicles. An improved method for liposome targeting, J. Biol. Chem. 257 (1982) 286–288.
[22] L. Nobs, F. Buchegger, R. Gurny, E. Allemann, Current methods for attaching targeting ligands to liposomes and nanoparticles, J. Pharm. Sci. 93 (2004) 1980–1992.
[23] M.K. Yu, J. Park, S. Jon, Targeting strategies for multifunctional nanoparticles in cancer imaging and therapy, Theranostics 2 (2012) 3–44.
[24] Y. Jiang, J. Chen, C. Deng, E.J. Suuronen, Z. Zhong, Click hydrogels, microgels and nanogels: Emerging platforms for drug delivery and tissue engineering, Biomaterials 35 (2014) 4969–4985.
[25] S.D. Fontaine, R. Reid, L. Robinson, G.W. Ashley, D.V. Santi, Long-term stabilization of maleimide-thiol conjugates, Bioconjug. Chem. 26 (2015) 145–152.
[26] J.D. Gregory, The stability of *N*-ethylmaleimide and its reaction with sulfhydryl groups, J. Am. Chem. Soc. 77 (1955) 3922–3923.
[27] J.L. Webb, N-ethylmaleimide, in: Enzyme and Metabolic Inhibitors, Academic Press, New York, 1966, pp. 337–365.
[28] C.P. Ryan, M.E. Smith, F.F. Schumacher, D. Grohmann, D. Papaioannou, G. Waksman, F. Werner, J.R. Baker, S. Caddick, Tunable reagents for multi-functional bioconjugation: reversible or permanent chemical modification of proteins and peptides by control of maleimide hydrolysis, Chem. Commun. 47 (2011) 5452–5454.
[29] O. Koniev, A. Wagner, Developments and recent advancements in the field of endogenous amino acid selective bond forming reactions for bioconjugation, Chem. Soc. Rev. 44 (2015) 5495–5551.
[30] S. Matsui, H. Aida, Hydrolysis of some N-alkylmaleimides, J. Chem. Soc. Perkin Trans. 2 (1978) 1277–1280.

[31] M. Oswald, S. Geissler, A. Goepferich, Determination of the activity of maleimide-functionalized phospholipids during preparation of liposomes, Int. J. Pharm. 514 (2016) 93–102.
[32] H.K. Makadia, S.J. Siegel, Poly lactic-co-glycolic acid (PLGA) as biodegradable controlled drug delivery carrier, Polymer 3 (2011) 1377–1397.
[33] F. Danhier, E. Ansorena, J.M. Silva, R. Coco, A. Le Breton, V. Preat, PLGA-based nanoparticles: an overview of biomedical applications, J. Control. Release 161 (2012) 505–522.
[34] R.A. Jain, The manufacturing techniques of various drug loaded biodegradable poly (lactide-co-glycolide) (PLGA) devices, Biomaterials 21 (2000) 2475–2490.
[35] R.C. Mundargi, V.R. Babu, V. Rangaswamy, P. Patel, T.M. Aminabhavi, Nano/micro technologies for delivering macromolecular therapeutics using poly(D,L-lactide-co-glycolide) and its derivatives, J. Control. Release 125 (2008) 193–209.
[36] S. Acharya, S.K. Sahoo, PLGA nanoparticles containing various anticancer agents and tumour delivery by EPR effect, Adv. Drug Deliv. Rev. 63 (2011) 170–183.
[37] J.S. Desgrosellier, D.A. Cheresh, Integrins in cancer: biological implications and therapeutic opportunities, Nat. Rev. Cancer 10 (2010) 9–22.
[38] K. Temming, R.M. Schiffelers, G. Molema, R.J. Kok, RGD-based strategies for selective delivery of therapeutics and imaging agents to the tumour vasculature, Drug Resist. Updat. 8 (2005) 381–402.
[39] R.M. Schiffelers, A. Ansari, J. Xu, Q. Zhou, Q. Tang, G. Storm, G. Molema, P.Y. Lu, P.V. Scaria, M.C. Woodle, Cancer siRNA therapy by tumor selective delivery with ligand-targeted sterically stabilized nanoparticle, Nucleic Acids Res. 32 (2004) e149.
[40] Y. Zhu, J. Zhang, F. Meng, C. Deng, R. Cheng, J. Feijen, Z. Zhong, cRGD-functionalized reduction-sensitive shell-sheddable biodegradable micelles mediate enhanced doxorubicin delivery to human glioma xenografts *in vivo*, J. Control. Release 233 (2016) 29–38.
[41] Y. Sun, C. Kang, F. Liu, Y. Zhou, L. Luo, H. Qiao, RGD peptide-based target drug delivery of doxorubicin nanomedicine, Drug Dev. Res. 78 (2017) 283–291.
[42] H. Chen, G. Niu, H. Wu, X. Chen, Clinical application of radiolabeled RGD peptides for PET imaging of integrin αvβ3, Theranostics 6 (2016) 78–92.
[43] M. Kijanka, F.J. Warnders, M. El Khattabi, M. Lub-de Hooge, G.M. van Dam, V. Ntziachristos, L. de Vries, S. Oliveira, P.M. van Bergen en Henegouwen, Rapid optical imaging of human breast tumour xenografts using anti-HER2 VHHs site-directly conjugated to IRDye 800CW for image-guided surgery, Eur. J. Nucl. Med. Mol. Imaging 40 (2013) 1718–1729.
[44] A.C. Wolff, M.E. Hammond, D.G. Hicks, M. Dowsett, L.M. McShane, K.H. Allison, D.C. Allred, J.M. Bartlett, M. Bilous, P. Fitzgibbons, W. Hanna, R.B. Jenkins, P.B. Mangu, S. Paik, E.A. Perez, M.F. Press, P.A. Spears, G.H. Vance, G. Viale, D.F. Hayes, Recommendations for human epidermal growth factor receptor 2 testing in breast cancer: American Society of Clinical Oncology/College of American Pathologists clinical practice guideline update, J. Clin. Oncol. 31 (2013) 3997–4013.
[45] G. Hassanzadeh-Ghassabeh, N. Devoogdt, P. De Pauw, C. Vincke, S. Muyldermans, Nanobodies and their potential applications, Nanomedicine 8 (2013) 1013–1026.
[46] M.M. Harmsen, H.J. De Haard, Properties, production, and applications of camelid single-domain antibody fragments, Appl. Microbiol. Biotechnol. 77 (2007) 13–22.
[47] R. Chakravarty, S. Goel, W. Cai, Nanobody: the "magic bullet" for molecular imaging? Theranostics 4 (2014) 386–398.
[48] S. Oliveira, R. Heukers, J. Sornkom, R.J. Kok, P.M. van Bergen En Henegouwen, Targeting tumors with nanobodies for cancer imaging and therapy, J. Control. Release 172 (2013) 607–617.
[49] M.F. Zambaux, F. Bonneaux, R. Gref, P. Maincent, E. Dellacherie, M.J. Alonso, P. Labrude, C. Vigneron, Influence of experimental parameters on the characteristics of poly(lactic acid) nanoparticles prepared by a double emulsion method, J. Control. Release 50 (1998) 31–40.
[50] N. Samadi, M.J. van Steenbergen, J.B. van den Dikkenberg, T. Vermonden, C.F. van Nostrum, M. Amidi, W.E. Hennink, Nanoparticles based on a hydrophilic polyester with a sheddable PEG coating for protein delivery, Pharm. Res. 31 (2014) 2593–2604.
[51] M.N. Khan, Kinetics and mechanism of the alkaline hydrolysis of maleimide, J. Pharm. Sci. 73 (1984) 1767–1771.
[52] S. Kirchhof, A. Strasser, H.J. Wittmann, V. Messmann, N. Hammer, A.M. Goepferich, F.P. Brandl, New insights into the cross-linking and degradation mechanism of Diels–Alder hydrogels, J. Mater. Chem. B 3 (2015) 449–457.
[53] R.M. Schiffelers, G.A. Koning, T.L. ten Hagen, M.H. Fens, A.J. Schraa, A.P. Janssen, R.J. Kok, G. Molema, G. Storm, Anti-tumor efficacy of tumor vasculature-targeted liposomal doxorubicin, J. Control. Release 91 (2003) 115–122.
[54] M.M. Kijanka, A.S. van Brussel, E. van der Wall, W.P. Mali, P.J. van Diest, P.M. van Bergen en Henegouwen, S. Oliveira, Optical imaging of pre-invasive breast cancer with a combination of VHHs targeting CAIX and HER2 increases contrast and facilitates tumour characterization, EJNMMI Res. 6 (2016) 14.
[55] J.S. Hrkach, M.T. Peracchia, A. Domb, N. Lotan, R. Langer, Nanotechnology for biomaterials engineering: structural characterization of amphiphilic polymeric nanoparticles by 1H NMR spectroscopy, Biomaterials 18 (1997) 27–30.
[56] G.D. Poe, W.L. Jarret, C.W. Scales, C.L. McCormick, Enhanced coil expansion and intrapolymer complex formation of linear poly(methacrylic acid) containing poly (ethylene glycol) grafts, Macromolecules 37 (2004) 2603–2612.
[57] A.J. de Graaf, K.W. Boere, J. Kemmink, R.G. Fokkink, C.F. van Nostrum, D.T. Rijkers, J. van der Gucht, H. Wienk, M. Baldus, E. Mastrobattista, T. Vermonden, W.E. Hennink, Looped structure of flowerlike micelles revealed by 1H NMR relaxometry and light scattering, Langmuir 27 (2011) 9843–9848.
[58] F. Danhier, B. Vroman, N. Lecouturier, N. Crokart, V. Pourcelle, H. Freichels, C. Jerome, J. Marchand-Brynaert, O. Feron, V. Preat, Targeting of tumor endothelium by RGD-grafted PLGA-nanoparticles loaded with paclitaxel, J. Control. Release 140 (2009) 166–173.
[59] Q. Xu, Y. Liu, S. Su, W. Li, C. Chen, Y. Wu, Anti-tumor activity of paclitaxel through dual-targeting carrier of cyclic RGD and transferrin conjugated hyperbranched copolymer nanoparticles, Biomaterials 33 (2012) 1627–1639.
[60] M. Kijanka, E.G. van Donselaar, W.H. Muller, B. Dorresteijn, D. Popov-Celeketic, M. El Khattabi, C.T. Verrips, P.M.P. van Bergen en Henegouwen, J.A. Post, A novel immuno-gold labeling protocol for nanobody-based detection of HER2 in breast cancer cells using immuno-electron microscopy, J. Struct. Biol. 199 (2017) 1–11.
[61] W. Yao, P. Xu, J. Zhao, L. Ling, X. Li, B. Zhang, N. Cheng, Z. Pang, RGD functionalized polymeric nanoparticles targeting periodontitis epithelial cells for the enhanced treatment of periodontitis in dogs, J. Colloid Interface Sci. 458 (2015) 14–21.
[62] A. Malzert, F. Boury, P. Saulnier, J.P. Benoit, J.E. Proust, Interfacial properties of mixed polyethylene glycol/poly(D,L-lactide-co-glycolide) films spread at the air/water interface, Langmuir 16 (2000) 1861–1867.
[63] C. Javiya, S. Jonnalagadda, Physicochemical characterization of spray-dried PLGA/PEG microspheres, and preliminary assessment of biological response, Drug Dev. Ind. Pharm. 42 (2016) 1504–1514.
[64] E. Vega, M.A. Egea, A.C. Calpena, M. Espina, M.L. Garcia, Role of hydroxypropyl-beta-cyclodextrin on freeze-dried and gamma-irradiated PLGA and PLGA-PEG diblock copolymer nanospheres for ophthalmic flurbiprofen delivery, Int. J. Nanomedicine 7 (2012) 1357–1371.
[65] J.M. Rabanel, P. Hildgen, X. Banquy, Assessment of PEG on polymeric particles surface, a key step in drug carrier translation, J. Control. Release 185 (2014) 71–87.
[66] S. Stolnik, B. Daudali, A. Arien, J. Whetstone, C.R. Heald, M.C. Garnett, S.S. Davis, L. Illum, The effect of surface coverage and conformation of poly(ethylene oxide) (PEO) chains of poloxamer 407 on the biological fate of model colloidal drug carriers, Biochim. Biophys. Acta 1514 (2001) 261–279.
[67] J.L. Perry, K.G. Reuter, M.P. Kai, K.P. Herlihy, S.W. Jones, J.C. Luft, M. Napier, J.E. Bear, J.M. DeSimone, PEGylated PRINT nanoparticles: the impact of PEG density on protein binding, macrophage association, biodistribution, and pharmacokinetics, Nano Lett. 12 (2012) 5304–5310.
[68] C.C. Lee, E.R. Samuels, The kinetics of reaction between L-cysteine hydrochloride and some maleimides, Can. J. Chem. 42 (1964) 168–170.
[69] P. Schelte, C. Boeckler, B. Frisch, F. Schuber, Differential reactivity of maleimide and bromoacetyl functions with thiols: application to the preparation of liposomal diepitope constructs, Bioconjug. Chem. 11 (2000) 118–123.
[70] L.-T.T. Nguyen, M.T. Gokmen, F.E. Du Prez, Kinetic comparison of 13 homogeneous thiol–X reactions, Polym. Chem. 4 (2013) 5527–5536.
[71] M.T. Gokmen, J. Brassinne, R.A. Prasath, F.E. Du Prez, Revealing the nature of thio-click reactions on the solid phase, Chem. Commun. 47 (2011) 4652–4654.
[72] C. Wischke, S.P. Schwendeman, Principles of encapsulating hydrophobic drugs in PLA/PLGA microparticles, Int. J. Pharm. 364 (2008) 298–327.
[73] F. Ramazani, W. Chen, C.F. van Nostrum, G. Storm, F. Kiessling, T. Lammers, W.E. Hennink, R.J. Kok, Strategies for encapsulation of small hydrophilic and amphiphilic drugs in PLGA microspheres: state-of-the-art and challenges, Int. J. Pharm. 499 (2016) 358–367.
[74] A. Vila, H. Gill, O. McCallion, M.J. Alonso, Transport of PLA-PEG particles across the nasal mucosa: effect of particle size and PEG coating density, J. Control. Release 98 (2004) 231–244.
[75] F. Boury, T. Ivanova, I. Panaiotov, J.E. Proust, A. Bois, J. Richou, Dynamic properties of poly(DL-lactide) and polyvinyl alcohol monolayers at the air/water and dichloromethane/water interfaces, J. Colloid Interface Sci. 169 (1995) 380–392.
[76] S.C. Lee, J.T. Oh, M.H. Jang, S.I. Chung, Quantitative analysis of polyvinyl alcohol on the surface of poly(D, L-lactide-co-glycolide) microparticles prepared by solvent evaporation method: effect of particle size and PVA concentration, J. Control. Release 59 (1999) 123–132.
[77] C.T. Sengel-Turk, C. Hascicek, A.L. Dogan, G. Esendagli, D. Guc, N. Gonul, Preparation and in vitro evaluation of meloxicam-loaded PLGA nanoparticles on HT-29 human colon adenocarcinoma cells, Drug Dev. Ind. Pharm. 38 (2012) 1107–1116.
[78] S.K. Sahoo, J. Panyam, S. Prabha, V. Labhasetwar, Residual polyvinyl alcohol associated with poly (D,L-lactide-co-glycolide) nanoparticles affects their physical properties and cellular uptake, J. Control. Release 82 (2002) 105–114.
[79] R. Gref, A. Domb, P. Quellec, T. Blunk, R.H. Muller, J.M. Verbavatz, R. Langer, The controlled intravenous delivery of drugs using PEG-coated sterically stabilized nanospheres, Adv. Drug Deliv. Rev. 16 (1995) 215–233.